

DOI: 10.1002/adma.200700584

## Snapping Surfaces\*\*

By Douglas P. Holmes and Alfred J. Crosby\*

The responsive mechanism of the Venus flytrap has captured the interest of scientists for centuries. Although a complete understanding of the mechanism controlling the Venus flytrap movement has yet to be determined, a recent publication by Forterre et al.<sup>[1]</sup> demonstrates the importance of geometry and material properties for this fast, stimuli-responsive movement. Specifically, the movement is attributed to a snap-through elastic instability whose sensitivity is dictated by the length scale, geometry, and materials properties of the features.<sup>[2]</sup> Here, we use lessons from the Venus flytrap to design surfaces that dynamically modify their topography. We present a simple, robust, biomimetic responsive surface based on an array of microlens shells that snap from one curvature (e.g., concave) to another curvature (e.g., convex) (Fig. 1) when a critical stress develops in the shell structure.

This snap-transition is due to the onset of an elastic, snap-through instability similar to the capture mechanism of the Venus flytrap. The response rates can be over two orders of magnitude faster than the typical response of shape-memory polymers, and the sensitivity and rate of the response can be tuned with predictable geometric and/or material property changes. Based on materials choice, a wide variety of external stimuli can trigger this stress development, such as temperature, pH, solvent swelling, magnetism, electric current, and light. This strategy has great potential for the design of responsive surfaces, which will impact a variety of applications including: release-on-command coatings<sup>[3]</sup> and adhesives,<sup>[4-7]</sup> on-command frictional changes,<sup>[8,9]</sup> instant modification of op-

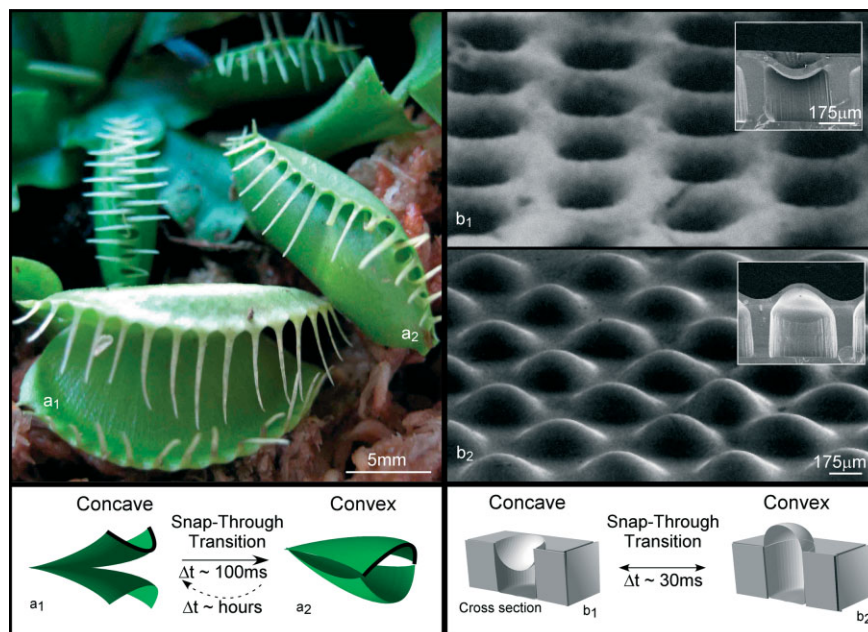


**Figure 1.** Snap-through of the Venus flytrap leaves from concave ( $a_1$ ) to convex ( $a_2$ ) occurs through the onset of an elastic instability. Our responsive surface of concave ( $b_1$ ) microlenses uses the same process to snap to a convex topography ( $b_2$ ) in  $\sim 30$  ms.

tical properties at an interface,<sup>[10,11]</sup> rapid response drug delivery,<sup>[12-14]</sup> chemical sensing,<sup>[15-17]</sup> and antimicrobial devices.<sup>[18]</sup>

To fabricate the active surface structures, we use the Euler buckling of plates to generate a controlled array of microlens shells under equibiaxial compressive stress (Fig. 2a). First, we pattern cylindrical posts of photoresist onto a silicon wafer and micromold poly(dimethyl siloxane) (PDMS) (Sylgard 184<sup>TM</sup>) elastomer onto it, creating an array of holes. This elastic, PDMS array of holes is then placed in equi-biaxial strain through a simple inflation procedure. A thin film of cross-linked PDMS (typically 15–60  $\mu\text{m}$  in thickness) coated with a thin ( $\sim 1$   $\mu\text{m}$ ) layer of uncured PDMS is placed on the surface of the strained holes. The assembly is heated to crosslink the uncured PDMS and bond the film to the array of holes while under equibiaxial tension. Releasing the tension causes an equibiaxial compressive strain to develop in the thin PDMS coating. The associated compressive stresses cause the circular plate of PDMS on the surface of each hole to buckle, thus creating an array of convex microlenses. This technique for microlens preparation is simple, robust, and should be scalable to much smaller length scales across a multitude of materials.

[\*] Prof. A. J. Crosby, D. P. Holmes  
Polymer Science & Engineering  
University of Massachusetts, Amherst  
120 Governors Dr. Amherst, MA 01003 (USA)  
E-mail: crosby@mail.pse.umass.edu

[\*\*] Funding for this work was provided by the Army Research Office Young Investigator Program. The authors thank Edwin P. Chan and Kyriaki Kalaitzidou for insightful discussions, and acknowledge NSF-MRSEC Central Facilities for use of their SEM, as well as Professor McCarthy's group for use of their oxygen-plasma cleaner.

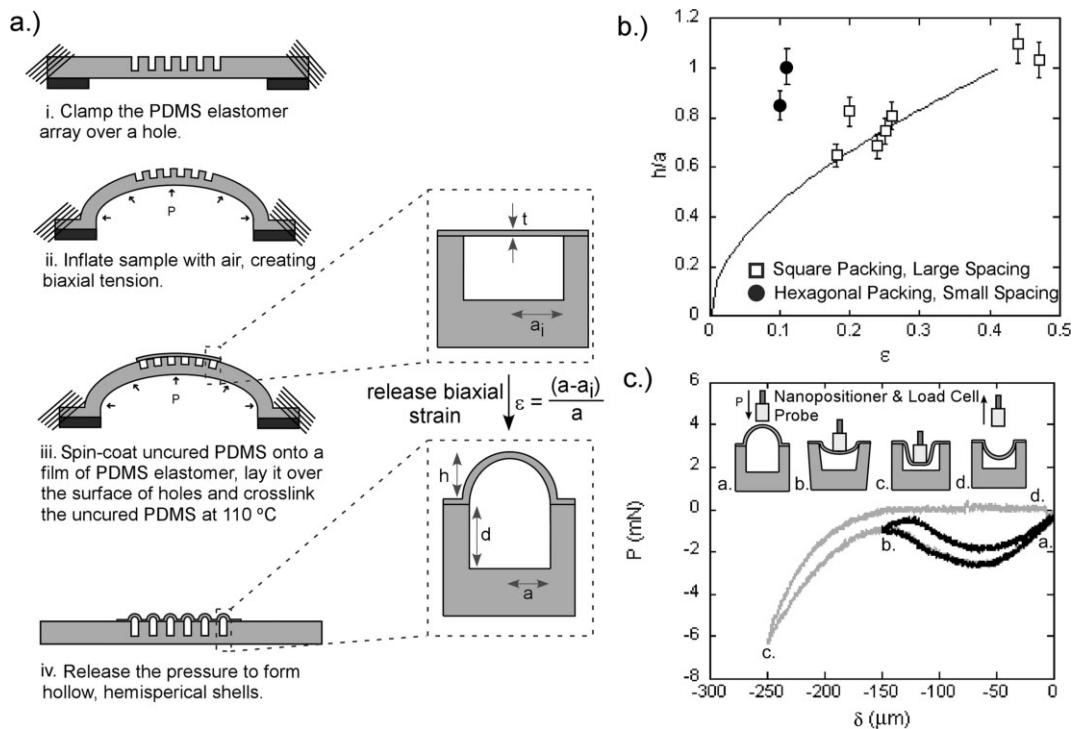


**Figure 2.** a) A schematic of the responsive interface preparation. b) A graph of  $h/a$  versus strain to illustrate predictable control of shell curvature. c) A schematic of using a concentrated point force to snap an individual shell, along with a force versus displacement plot illustrating the critical force of snap-through.

As a first estimate, the curvature of the microlenses can be predicted by a conservation of surface area, where the cross-sectional area of the hole under equibiaxial tension should equal the surface area of the resultant spherical shell. While the critical stress that develops from the applied biaxial compression dictates the formation of lenses and is dependent on the film thickness and material properties, the critical strain for formation is independent of material properties and thickness. Accordingly, the geometry of the microlenses produced in our experiments was independent of film thickness for the limited range measured (15 to 60  $\mu\text{m}$ ). Therefore, for a mechanically uncoupled shell, the ratio of the amplitude of the shell to the radius of the hole is proportional to the applied strain (Fig. 2b), where  $a$  is the unstrained radius of the hole,  $\epsilon$  is the applied strain, and  $h$  is the shell's amplitude:

$$\frac{h}{a} = \sqrt{\epsilon(2 + \epsilon)} \quad (1)$$

As the spacing of shells decreases, the relationship of  $h/a$  deviates from this surface area conservation (Fig. 2b). We attribute this effect to the influence of the shell spacing due to mechanical coupling effects, which are unaccounted for in our simple model.

To control the transition from convex to concave curvature, the stress in the shell structure must be controlled. As described in the continuum mechanics of shell structures, at a

critical applied stress an elastic instability will occur,<sup>[19]</sup> similar to Euler buckling of a beam. This critical stress is determined by the balance of geometric and mechanical properties.<sup>[19]</sup> As one example, individual shells can be snapped by applying a concentrated point force greater than or equal to ~6 mN to the shells (Fig. 2c). To initiate this snap-through, we brought a cylindrical probe (radius = 85  $\mu\text{m}$ ) connected to a load cell and nanopositioner into contact with the apex of a single microlens. Applying a force below the critical force caused the shell to reversibly return to the convex geometry (black data). If the critical concentrated force is applied the shells snap to the concave state and remain there upon removal of the probe (gray data). This change is indicated by the contact force ( $P$ ) changing to zero at a displacement ( $\delta$ ) of -150  $\mu\text{m}$ .

Alternatively, if a trigger mechanism is used to develop the critical stress in all shells simultaneously, then the entire surface of shells will change curvature (Fig. 1b). One way to achieve this switching of multiple lenses from convex to concave is by exposing the responsive surface to oxygen plasma treatment. The exposure of the surface to oxygen plasma leads to a conversion of the organo-silicon surface to silicon oxides.<sup>[20]</sup> This conversion process causes a volumetric decrease on the surface of the PDMS film, triggering the shells to snap from convex to concave to minimize the development of tensile stresses in the outer surface layer.

To snap the shells from concave to convex, a triggering mechanism that causes volumetric expansion can be used. We

have demonstrated a simple mechanism by swelling our elastic network with an organic solvent to develop an osmotic stress, similar to the Venus flytrap mechanism. Hexane was introduced to our PDMS surface, swelling the crosslinked network (Fig. 3a). The hexane can quickly diffuse through the thin silica layer on the surface ( $\sim 10$  nm)<sup>[20]</sup> created by exposure to oxygen-plasma. As the surface swells, it expands initially until a compressive stress is generated due to the lateral confinement from the edges of each hole (Fig. 3b, where  $\lambda_{tr}$  describes the lateral biaxial strain of the hole). This compressive stress leads to a growth of higher buckling modes until a critical strain is reached. At this critical value, the shell undergoes a snap-through transition to the more stable convex state. A complete description of the shell mechanics through this transition has not been accomplished yet and reference to developed analytical solutions is not possible due to the complex boundary conditions. Nonetheless, this transition in stress state can be associated with volumetric expansion in the buckled film, a mechanism that can be associated with a variety of other environmental changes (pH, light, temperature, etc.).

A distinguishing advantage of shell structures, as illustrated with our surfaces, is the tendency to transition through a “snap” instability. “Snap” instabilities differ from smooth elastic instabilities in their ability to undergo large magnitude

geometric changes through short timescales. The transition from this pre-snap, largely concave state to the post-snap, convex state in our shell surfaces (with a thickness of  $35 \mu\text{m}$ ) takes approximately 30 ms (note: the timescale measurement is limited by the resolution of our camera at 30 frames per second). As in the Venus flytrap, the timescale for this snap-through transition is dictated by the smallest length scale in the system, in this case by the thickness of the shell.<sup>[1]</sup> The timescale for the snap-through of the Venus flytrap,  $\tau_p \approx 100$  ms, is governed by:<sup>[1,21,22]</sup>

$$\tau_p \approx \frac{\mu t^2}{kE} \quad (2)$$

where  $\mu$  is the viscosity of the swelling fluid,  $t$  is the film thickness,  $k$  is the hydraulic permeability, and  $E$  is Young’s modulus. The transition time for the snapping surface shells also obeys this scaling. To demonstrate this, we plot the snap transition time as a function of shell thickness (Fig. 3c). The predicted trendline is based on a measured elastic modulus ( $E = 4$  MPa) and literature values for the permeation of hexane through PDMS<sup>[23]</sup> ( $\mu/k \sim 10^{-14} \text{ m}^2 \text{ Pa}^{-1} \text{ s}^{-1}$ ). This suggests that the rate of the snap transition is predictably tuned with the geometry and material properties of the shell structures.

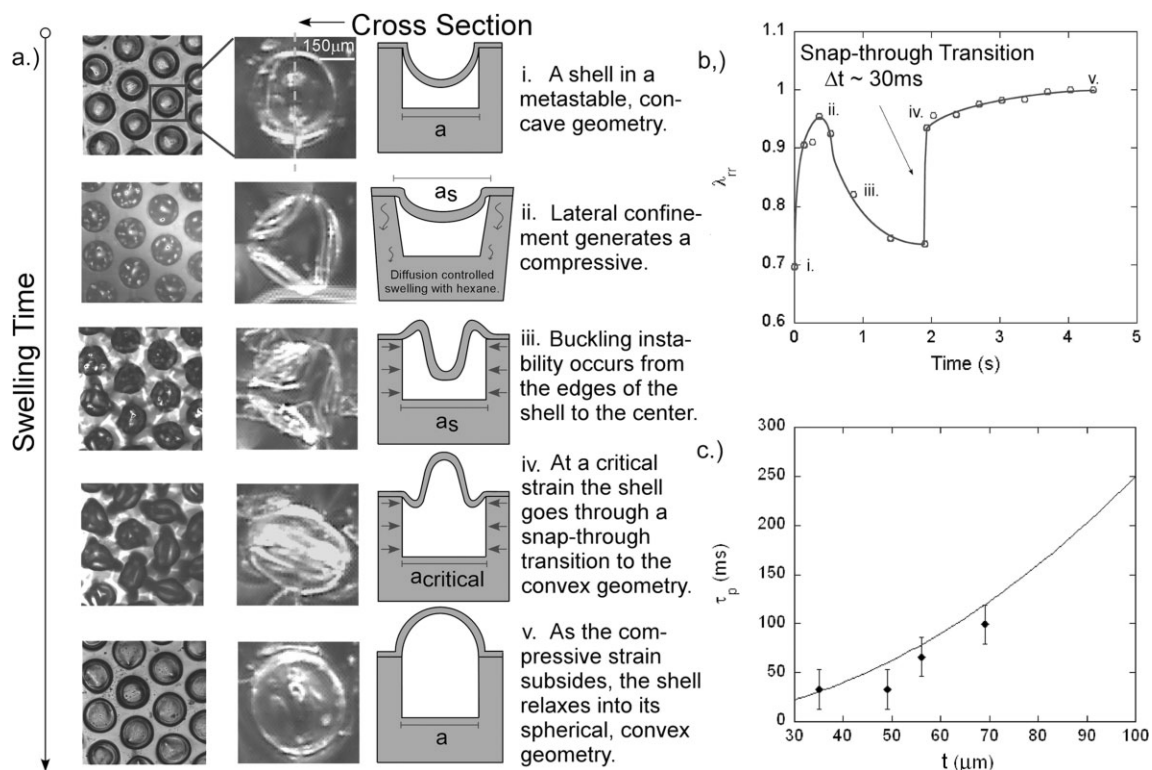


**Figure 3.** a) Images of the responsive surface snap-through process as well as a schematic illustrating the snap-through transition of a single shell from concave to convex. The triggering mechanism is the development of osmotic stress, similar to the triggering mechanism observed in the Venus flytrap. The development of osmotic stress in our system is due to the swelling of the PDMS network with hexane. b) A corresponding strain versus time graph illustrating the snap-through transition. c) A plot of snap-through time versus film thickness.

Designing a surface that undergoes snap, not smooth, instability transitions is also linked to the balance of materials properties and geometry. Forterre et al.<sup>[1]</sup> showed that a dimensionless geometric parameter  $a = a^4/R^2 t^2$  determines the nature of closure for the Venus flytrap leaves as either snapping or smooth closure,<sup>[1]</sup> where  $R$  is the radius of curvature, and  $a$  and  $t$  were defined above. They determined that  $a > 0.8$  was necessary for leaf snapping. Similarly, this transition in the context of classical shell mechanics, a dimensionless parameter  $\xi = h/t$  can be used for spherical shell under fixed edge conditions. For this boundary constraint,  $\xi$  must exceed a value of 2. While neither parameter completely describes the boundary conditions of the microlenses presented here, they represent lower limits required for shell snap-through. Our shell geometry has values of  $a$  (19.0) and  $\xi$  (3.7) which greatly exceed the previously-mentioned critical values of both  $a$  and  $\xi$ .

As an initial demonstration of a responsive property of these surfaces, we illustrate the utility of these surfaces as responsive microlens arrays for optical display applications. In a convex state, the assembled shell structures form a functional microlens array (Fig. 4) with a focal point above the structure surface. Upon transitioning to a concave curvature, the focal

point of the shell structures is changed to beneath the shell surface (Fig. 4). These transitions can occur locally (single lenses) or over the entire microlens array depending upon the spacing, material properties, and specific nature of the triggering mechanism. In addition to optical properties, the controlled, responsive topographical changes can be used to alter a wide range of properties from friction to wetting.

In summary, we have presented a biomimetic responsive interface that changes topography over a large length scale and small time scale by transitioning through an elastic instability. The snap-through transition is dictated by geometry, and materials properties, thus the transition time, triggering sensitivity, and magnitude change are highly tunable. Surface topography changes over this time scale have the potential to impact many applications, including sensors,<sup>[15-17]</sup> antimicrobial coatings,<sup>[18]</sup> adhesives,<sup>[3-7]</sup> friction modifiers,<sup>[8,9]</sup> optical devices,<sup>[10,11]</sup> and drug delivery systems.<sup>[12-14]</sup> We have illustrated their potential use as a rapidly switchable optical device by changing the focal properties of the microlens shells upon triggering a snap-transition. The fabrication method is robust and should be scalable to smaller length scales and a variety of other materials systems.

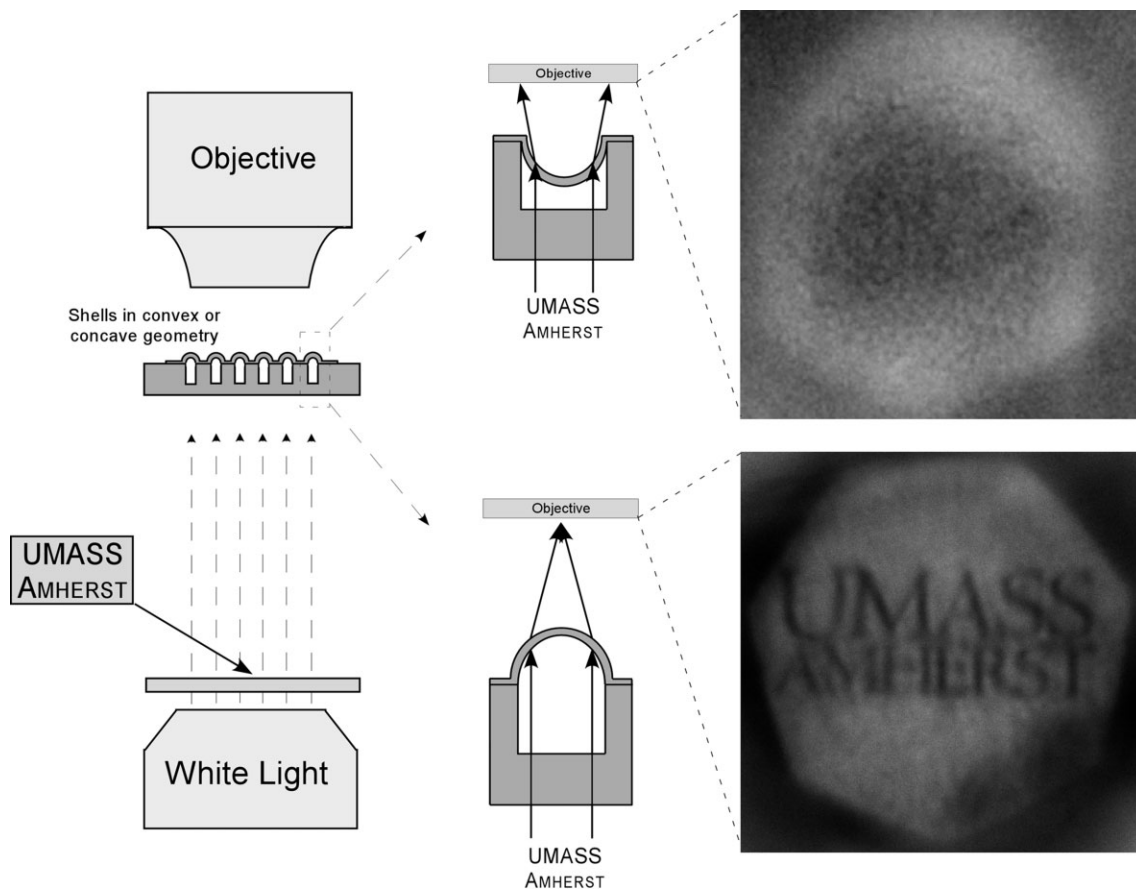


**Figure 4.** Demonstration of optical functionality of microlens shells and their ability to change focal properties upon triggering. In the arrangement illustrated schematically on the left, no image is projected onto the objective when the shell curvature is concave. Upon triggering, the shell transitions to convex and an image is focused at the focal point of the microscope objective.

## Experimental

An SU-82100 negative photoresist (Microchem<sup>®</sup>) was deposited by spin-coating at 1000 rpm for 1 min onto a clean silicon wafer. The resist was then pre-baked at 90 °C for 10 min exposed for 70 s (OAI 500W DUV, intensity = 20 mJ cm<sup>-2</sup>) with a mask of circles prepared by Pageworks (Cambridge, MA). The exposed resist was post-baked at 90 °C for 1 min and developed in SU-8 Developer (Microchem<sup>®</sup>) for 10 min to reveal cylindrical posts with a height of 244 μm.

Crosslinked PDMS films are prepared by thoroughly mixing Dow Corning Sylgard<sup>™</sup> 184 oligomer with catalyst (10 to 1 by weight) and then degassing under vacuum for 1 hour. The degassed mixture was cast onto the cylindrical photoresist posts and cured at 110 °C for 30 min to yield 1.5 mm thick PDMS films with 244 μm holes on the surface.

The crosslinked PDMS film with surface holes is clamped over a circular hole and inflated. This places the PDMS film in an approximate equibiaxial strain which is quantified by measuring the original and strained dimensions of the surface holes by optical microscopy (Zeiss, Variotech). A thin film of crosslinked PDMS ( $h = 15\text{--}60\ \mu\text{m}$ ) is placed on top of the array of inflated holes with a thin layer of uncrosslinked PDMS at the interface between the two layers. The sample is then heated at 110 °C for 30 min to allow the remaining uncrosslinked PDMS to cure while the substrate is inflated. The pressure is released, thus compressing the thin film and creating the spherical shells on the surface. A Harrick Plasma Cleaner (PDC-001) is used for exposure to oxygen plasma for a fixed time of 30 s.

The height of the microlenses was characterized by reflective mode optical microscopy (Zeiss, Axiovert). Optical projection through the microlenses was performed by transmission mode optical microscopy (Zeiss, Axiovert). Geometry of the convex and concave shells was examined by scanning electron microscopy (JOEL 6320FXV FESEM, SEI mode, 10 kV, gold-coated). A replica of the concave shells was prepared for examination by SEM to prevent the vacuum of the microscope from snapping the shells to the convex geometry. The microlenses were swelled with hexane (VWR) and observed via optical microscopy.

Received: March 8, 2007  
Revised: April 19, 2007

- [1] Y. Forterre, J. M. Skotheim, J. Dumais, L. Mahadevan, *Nature* **2005**, 433, 421.
- [2] J. M. Skotheim, L. Mahadevan, *Science* **2005**, 308, 1308.
- [3] B. Bhushan, R. A. Sayer, *Microsyst. Technol.* **2007**, 13, 71.
- [4] A. J. Crosby, M. Hageman, A. Duncan, *Langmuir* **2005**, 21, 11 738.
- [5] T. Thomas, A. J. Crosby, *J. Adhes.* **2006**, 82, 311.
- [6] K. Autumn, A. M. Peattie, *Integr. Comp. Biol.* **2002**, 42, 1081.
- [7] B. Bhushan, A. G. Peressadko, T. W. Kim, *J. Adhes. Sci. Technol.* **2006**, 20, 1475.
- [8] M. K. Chaudhury, M. J. Owen, *Langmuir* **1993**, 9, 29.
- [9] P. L. Menezes, Kishore, S. V. Kailas, *Tribol. Lett.* **2006**, 24, 265.
- [10] L. Dong, A. K. Agarwal, D. J. Beebe, H. R. Jiang, *Nature* **2006**, 442, 551.
- [11] A. Werber, H. Zappe, *Appl. Opt.* **2005**, 44, 3238.
- [12] K. E. Urich, S. M. Cannizzaro, R. S. Langer, K. M. Shakesheff, *Chem. Rev.* **1999**, 99, 3181.
- [13] R. Langer, *Nature* **1998**, 392, 5.
- [14] R. Langer, *Science* **1990**, 249, 1527.
- [15] A. N. Shipway, E. Katz, I. Willner, *ChemPhysChem* **2000**, 1, 18.
- [16] J. Kong, N. R. Franklin, C. W. Zhou, M. G. Chapline, S. Peng, K. J. Cho, H. J. Dai, *Science* **2000**, 287, 622.
- [17] J. H. Holtz, S. A. Asher, *Nature* **1997**, 389, 829.
- [18] K. Lewis, A. M. Klibanov, *Trends Biotechnol.* **2005**, 23, 343.
- [19] D. Shilkrut, *Stability of Nonlinear Shells*, Elsevier, London **2002**.
- [20] J. T. Koberstein, *MRS Bull.* **1996**, 21, 19.
- [21] M. A. Biot, *J. Appl. Phys.* **1941**, 12, 155.
- [22] J. M. Skotheim, L. Mahadevan, *Proc. R. Soc. London Ser. A* **2004**, 460, 1995.
- [23] *Polymer Data Handbook*, Oxford University Press, Oxford **1999**.